出國報告（出國類別：會議）

赴法參加 2008 年世界分子影像年會及發表論文

服務機關：原子能委員會
姓名職稱：諮議會陳浩然副執行秘書
張志賢副研究員
派赴國家：法國
出國期間：96 年 9 月 8 日起至 96 年 9 月 14 日
報告日期：96 年 10 月 17 日

摘　要

本次公差，主要是本所陳浩然博士、張志賢博士等二員，奉派赴法國尼斯，公差目的爲參加2008年世界分子影像年會「2008 World Molecular Imaging Congress」，此爲一年一度分子影像在醫學應用之盛會，今年第一次由美國分子影像學會、美國分子影像協會、歐洲分子影像學會、世界磁振造影學會、北美放射學會、美國核醫學會、歐洲生醫影像中心及亞洲分子影像聯合學會等美洲、歐洲及亞洲學會首次舉辦聯合年會。會議內容主要爲探討活體細胞、腫瘤等疾病之分子影像，新核醫藥物合成、標幟及細胞動物分子造影應用之最新進展，參加此會議有助於了解活體中生物反應之進行，參與本次會議對核研所正在進行之研發計畫有很大助益。

Abstract

The aim of business travel by Dr. Haw-Jan Chen and Dr. Chih-hsien Chang was to attend the 2008 World Molecular Imaging Congress in Nice, France. The conference this year was hold by many societies and associations in the world, including Society for Molecular Imaging (SMI), Academy of Molecular Imaging (AMI), European Society of Molecular Imaging (ESMI), International Society for Magnetic Resonance in Medicine (ISMRM), Radiological Society of North America (RSNA), Society of Nuclear Medicine (SNM), European Institute for Biomedical Imaging Research (EIBIR) and Federation of Asian Societies of Molecular Imaging (FASMI). The contents of the conference include molecular imaging of cells and tumors, synthesis and labeling of new radiopharmaceuticals, molecular imaging in animal models. There are many benefits for research and developing projects in Institute of Nuclear Energy Research after attending the symposium.

目　　次

摘　要

（頁碼）

一、目　的 · 1

二、過　程 · 2

三、心　得 · 7

四、建　議　事　項 · 13

五、附　圖 · 14

六、附　錄 · 21

　　會議議程

一、 目 的

本次赴美公差目的有三，首先爲參加 2008 年世界分子影像年會「2008 World Molecular Imaging Congress」，會議內容主要爲探討活體細胞、腫瘤等疾病之分子影像，新核醫及細胞動物分子造影應用之最新進展，了解國際在核醫分子影像研究開發及應用之現況，作爲本所核醫研發計畫之依據及參考；第二爲發表論文，核研所此次有十一篇論文經大會接受發表，前往國際會議發表論文，有助宣揚核研所的研發成果；第三是於會場直接和世界相關核醫及分子影像專家交換意見，並檢討國內核醫分子影像研發現況及方向，參與本次會議正在進行研發之計畫有很大助益。

二、 過程

(一) 本次公差行程如下:

日期	星期	地點	內容
9 月 8-9 日	一二		去程：台北至法國尼斯
9 月 10-13 日	三-六	尼斯	參加 2008 年世界分子影像年會「2008 World Molecular Imaging Congress」
9 月 13-14 日	六-日		返程：法國尼斯至台北

(二) 會議內容

於法國尼斯召開的 2008 年世界分子影像年會爲一年一度分子影像在醫學應用之盛會，今年第一次由美國分子影像學會(Society for Molecular Imaging, SMI)、美國分子影像協會(Academy of Molecular Imaging (AMI)、歐洲分子影像學會(European Society of Molecular Imaging, ESMI)、世界磁振造影學會(International Society for Magnetic Resonance in Medicine, ISMRM)、北美放射學會(Radiological Society of North America, RSNA)、美國核醫學會(Society of Nuclear Medicine, SNM)、歐洲生醫影像中心(European Institute for Biomedical Imaging Research, EIBIR) 及亞洲分子影像聯合學會(Federation of Asian Societies of Molecular Imaging, FASMI)等美洲、歐洲及亞洲學會首次舉辦聯合年會。

本次會議有來自 40 國家的 2100 位科技人員參加，會議共有 1148 論文發表，台灣除核研所外，尚有台大、三總、陽明、榮總、慈濟、北醫、高醫及長庚等單位研究人員近三十餘位參加。本次會議內容主要包含探討活體細胞、腫瘤等疾病之分子影像、新核醫藥物合成、標幟及細胞動物分子造影應用，腫瘤、腦神經及心血管疾病各領域中的之最新進展，會議重點方向爲診療機制之分子影像研究，其中核醫影像使用之同位素以 F-18、I-123、C-11 及 Cu-64 爲主，除了核醫影像之外，包含磁振造影(MRI)、Optical Imaging(螢光、冷光)、X-CT、Ultra-sound 等非核醫影像。其中已有許多結合 MRI-PET 的研究，MRI 與 Optical Imaging 之分子影像研究亦有許多報告，這些有益於本所多功能分子影像技術之整合，參與會議對本所正在進行研發計畫及臨床前動物實驗技術有很大助

益。

此次會議議程主要分兩部份：(1) 高等分子影像教育學程；(2) 世界分子影像年會。高等分子影像教育學程主要是高等分子影像教育，主要是介紹分子影像方面的最新進展，包含(a)活體藥理影像量化(Quantitative In vivo Pharmacological Imaging)；(b)細胞標誌方法 (Cell Labelling Methodalogies)；(c)體外分子影像分析(In vitro Molecular Imaging Assay)；(d) MRI/PET 組合科技(e)血管分子造影(Molecular Imaging Vascular Imaging)；(f)中樞神經放射藥物發展之造影 (Radiopharmaceuticals for Molecular CNS Imaging)； (d)神經疾病的活體幹細胞造影 (In-vivo Imaging of Stem Cells in Neurological Diseases 等。在分子影像年會部分主要爲(a) 幹細胞造影 (Imaging of Stem cells)；(b)新腫瘤探針之發展(New Cancer Probes Development)；(c)基因表現之造影 (Imaging Gene Expression)；(d)心血管造影 (Cardiovascular Imaging)；(e)神經分子影像(Molecular Neuroimaging)；(f)神經科學之分子影像 (Imaging in Neuroscience) (g)神經退化疾病的分子影像(Molecular Imaging of Neurodegenerative Diseases)；等 (議程如附件一)。

輻應中心共有十一篇論文經大會接受發表，前往國際會議發表論文，與相關領域學者討論，有助國際了解核研所的研發成果。論文題目分別如下:

1.Comparative Dosimetry and micro-SPECT/CT imaging of Nanotargeted ^{188}Re-(DXR)-Liposome in a C26 colon carcinoma mouse model。

2. [DTPA^{1}(^{99m}Tc(CO)$_3$), Lys^{3}, Tyr^{4}]Bombesin Biodistribution and SPECT/CT Imaging in SCID Mice with/without Receptor Blockade。

3. Biological Evaluation and microSPECT/CT imaging of ^{111}In-DTPA- Bombesin in PC-3 bearing SCID mice。

4. Evaluate the Effect of X-911 on LL2 Lung Tumor Bearing Nude Mice by Small Animal PET Imaging。

5. Tc-99m-ECD brain image on B6 stroke mice animal model by small animal multi-pinhole SPECT。

6. Auto-Synthesis and Research Study in Alzheimer's disease with [18F]-FDDNP。

7. Study of maximum-acceptance-angle effects in positron emission mammography

system。

8. Evaluation of image restoration methods for ^{188}Re quantitative micro-SPECT imaging。
9. Quantitative 3D Micro-SPECT Imaging of 188Re-BMEDA-Liposome in a C26 murine colon carcinoma solid tumor animal model。
10. 3D Automatic Quantitative Technique Apply to Osteoporosis Mice Study using Micro-CT Image。
11. Feasibility Study of a novel POI Imaging Detector for Dedicated Positron Breast Camera。

在腦神經研究方面，許多藥廠積極投入中樞神經系統疾病相關的診療藥物研發計畫；本次會議有數篇針對，這些研發經驗對於核研所有其重要參考價值。有關阿滋海默氏症的診斷最令人注目的是F-18-AV-45的臨床試驗案，F-18-AV-45最早是由賓州大學孔教授實驗室所開發，並由其團隊創立的Avid Radiopharmaceuticals, Inc.接續其臨床試驗，F-18-AV-45主要是與Amyloid plaque結合，做爲早期診斷Alzheimer's disease (AD)的造影試劑。此試劑能在一小時內快速與腦中β-Amyloid結合。目前已在美國進行第二期臨床試，驗並準備向FDA申請新藥上市（New Drug Application）；本研究利用10位AD病人，6位健康人進行F-18-AV-45 注射後90分鐘動態造影，SUVR結果顯示病人前葉皮層（front Cortex）及precuneus (PC)對F-18-AV-45之吸收遠高於正常人。因此18F-AV-45是有效、安全的AD早期診斷造影劑，其在腦中放射度活度在50～60分鐘即達到飽和（radioactivity plateau）。

腫瘤細胞爲了生長與轉移而具有許多生理特徵(圖一)，腫瘤的血管新生與腫瘤的成長及轉移有極大的關係，故抑制腫瘤新生血管的生成，成爲治療實質腫瘤的新方法之一。血管內皮生長因子(vascular endothelial growth factor，VEGF)是目前已知最有效且最具特異性地促進血管新生的因子之一。腦部血管病變是相當常見的疾病，血管病變所致的死亡人數中，腦僅次於心臟，而且腦血管病變所致的後遺症相當嚴重，其併發症如心肌梗塞等，經常導致殘障。一旦缺乏血流供應，腦細胞迅速死亡，殘存的細胞通常不足以維持正常功能。因此瞭解在發育及疾病過程之中，腦與其血管的密切關係就變得十分重要。由於近幾年來，血管新生與神經疾病分子機轉的相關研究進展快速，因此探究腦

的血管新生與神經疾病的關連正是時候。在神經病變的過程中，血管新生（angiogenesis）與神經細胞新生（neurogenesis）兩者都相當明顯。在血管新生、神經細胞新生與神經病變三者之間，血管內皮生長因子（vascular endothelial growth factor，VEGF）扮演了關鍵性的角色。VEGF 最初發現於血管系統，其相關的訊息傳遞也已清楚。近幾年來 VEGF 在神經系統的角色日漸顯著。從它在 stroke 及 motor neuron diseases 等神經病變的角色來看，VEGF 及其下游的訊息傳遞可能是這些疾病具有厚望的治療標的。

在腦造影與心血管造影研究方面，心肌梗塞的病人中發現血管內皮生長因子(VEGF)會過量表現(overexpression)，而在臨床治療上，中風後有 25%的病人在 3 年內會再發，急性心肌梗塞後，對這些病人可以考慮使用 VEGF 來預防中風。因此對於心血管疾病，利用分子影像來進行診療亦扮演重要的角色。

在腫瘤研發方面，蛙皮素（Bombesin, BBN）需與動物體內之胃泌素受體(BN/GRPR)受體結合發揮生理作用，胃泌素受體在攝護腺癌 (prostate cancer)、小細胞肺癌（small-cell lung cancers）、乳癌（breast cancer）腫瘤細胞上有過量分布；本次大會中共有十篇討論胃泌素受體及其造影劑論文發表，本次會議中 Dr. Mansi 發展出兩條 In-111 Bombesin Receptor antaganist，分別爲"In-111-RM25"及"In-111-RM27"，其中兩種藥物在 PC-3 攝護腺腫瘤研究中，在 4 小時有近 10 % ID/g 之吸收。In-111-RM27 在胰臟有高達 39.4 % ID/g 之吸收。此一現象代表藥物在體內維持高活性與穩定性。

在 Multimodality Molecular Imaging 與放射治療整合方面，華盛頓大學利用 ^{177}Lu-LS308 (RGDfk) peptide-DTPA 及遠紅外光染劑進行放射治療，並利用不同的造影系統來追蹤療效評估之結果；在荷有 4 tl/uc 腫瘤的小鼠，可利用冷光與遠紅外光系統來進行腫瘤的定位及藥物分析，^{177}Lu-LS308 則可用來研究治療性藥物的分佈與療效評估，此多功能分子影像也是本所未來發展的目標(圖二)。

在放射治療方面，德州大學聖安東尼奧校區(The University of Texas Health Science Center at San Antonio)發表 Re-186-PEG-liposomal doxorubicin (PLD)研究成果，該校區影像中心設施包含 Concorde microPET 及 Gamma-medica microSPECT/PET/CT，並包含

Optical imaging 非放射性同位素造影系統等；其菲力普(Phillips, William)教授在放射性同位素標幟微脂體已有十多年之經驗，其實驗室最著名的成就之一在於建立以 BMEDA (N,N-bis(2-mercaptoethyl)-N',N'-diethylethylenediamine) 配位子爲媒介進行 Tc-99/Re-188-liposome 標幟技術，使得放射性同位素 Re-188 能夠有效包埋於微脂體中，並在生物體中亦能穩定存在而不會分解或解離。在 Tc-99m-BMEDA-liposome 之大鼠造影研究中，可見 Tc-99m-BMEDA-liposome 體內滯留時間比 Tc-99m-BMEDA 久。

研究團隊成員 Goins 教授(Beth A. Goins)參加此一會議，研究團隊早在 2003 年建立 Re-186-BMEDA-liposome 標幟技術，其實驗證明血中穩定性良好，並研究其生物體分佈試驗及其 SPECT 造影，結果能有效看到 Re-186-liposome 有效延長體內滯留時間；此一研究爲放射性同位素標幟微脂體作爲放射治療之構想開了一扇大門，在此次的研討會中，他亦發表其研究團隊在此領域實驗之最新進展，他們使用頭頸癌的大鼠的裸鼠動物模式，證明放療加化療的治療結果最好(圖三)；目前 Gamma-medica microSPECT/PET/CT 儀器到位之後，研究團隊已同時進行解剖性造影(Functional Imaging)及功能性造影(Anatomical Imaging)。從 Re-186-PEG-liposomal doxorubicin (PLD)研究成果中可看到他們已朝放療加化學治療之組合性治療方向進行相關實驗。

Molecular Imaging and Translational Research Program 亦是本次會議討論重點之一，以往藥物上市需經臨床 phase I、II、III 耗時，此計劃主要是將臨床前動物試驗有潛力的藥物，直接進行人體臨床試驗以驗證其藥效。這個觀念已獲得美國與歐盟採納，飛利浦公司近年已成立轉譯影像中心，以縮短新藥研發至上臨床的時間(圖四)；Philips 近年已成立轉譯分子影像部門，主要研究基地設於荷蘭，從化學合成實驗室、放射化學實驗室、分子生物與細胞實驗室、臨床前分子影像實驗室等，其合作的對象包含：美國、歐洲、印度、中國等大學、研究機構與醫學中心，結合該公司在臨床前與醫用分子影像設備的優勢進行藥物開發。由飛利浦公司之轉譯影像中心架構了解分子影像之重要性，相信不久的未來轉譯影像中心亦將成爲產業界藥物開發之利器(圖五)。

三、心得

過去十年來世界活體分子影像(in-vivo molecular imaging)研究與應用快速發展與成長。活體分子影像可以提供活體生物系統(biology system)分子與遺傳功能層次正常與不正常細胞過程(cell process)之觀察與資訊，有利於人類疾病早期正確診療與基因体醫學及新藥之加速開發；由於分子影像之發展，顯現活體分子遺傳細胞行爲與過程，對細胞、組織與器官功能、動物模式研究及人類疾病的瞭解與核醫研究及臨床應用之重要性，歐美核子醫學界積極推動功能與分子影像研究與應用，毫無疑問將使核醫專家掌握創新醫學診斷與治療技術，邁向分子醫學研究與臨床應用發展之前驅。近年來，全球新藥研發在奈米技術的協助下，進而朝向藥物傳輸系統與主動標的傳輸系統的趨勢，即經由標的小分子（Ligand）辨識體內特定之受體（Receptor）像腫瘤細胞，而完成主動標的給藥的目的；因此本次會議包含此趨勢探討基因治療、免疫學、疫苗、癌症治療、臨床應用、影像分析等研發進展與應用。

分子影像之重要與受到重視可由許多方面看出，歐洲核醫雜誌已於 2002 年正式改名爲”European Journal of Nuclear Medicine and Molecular Imaging”。美國 2002 年第 49 屆核醫年會宣佈 SNM 新標幟爲”SNM & Advancing Molecular Imaging”，美國東岸與西岸分別於 2002 年成立美國分子影像學會(Society for Molecular Imaging) 與美國分子影像協會(Academy of Molecular Imaging)。 而 2007 年爲了匯集更多的專家與學者共同進入與分享分子影像的研究成果，因而此兩大學會共同舉辦「聯合分子影像年會」，由參與人數之多也了解分子影像在醫學研究與新藥開發之重要性；在 2008 年更進一步結合美國分子影像學會、美國分子影像協會、歐洲分子影像學會、世界磁振造影學會、北美放射學會、美國核醫學會、歐洲生醫影像中心及亞洲分子影像聯合學會等美洲、歐洲及亞洲學會首次舉辦世界分子影像年會，可之分子影像在醫學研究與新藥開發的重要性。

平均而言，在治療性新藥開發上，藥廠需時 10~12 年，花費 8~17 億美元，而暢銷藥上市後則是預期可達到每年 9 億美元的銷量。許多暢銷藥每年已銷售達 10-30 億美元。在發展診斷性影像的新藥時，平均而言，需時 8~10 年，花費 1~2 億美元。而已在

市場上銷售的診斷性造影藥則是已銷售達每年 2~4 億美元，分子影像加入藥物研發過程將縮短藥物開發時程與減少開發成本(圖六)。

Re-188、Re-186 爲放射出 β-射線，可做爲標靶治療腫瘤放射性同位素，因它們同時含 155 KeV 及 139 KeV γ-ray，故同時具備加馬造影診斷功能。它的物理性質如表：

表 銖-188 與銖-186 物理性質

Radionuclide	Physical half-life ($T_{1/2}$)	Mode of decay	γ-ray		β-ray			
			Energy (MeV)	Abundance (%)	Energy (MeV)		Range in tissue(mm)	
					Max.	Ave.	Max.	Ave.
^{188}Re	16.98 h	β^- (100)	0.155	14.9	2.12	0.765	11	3.5
^{186}Re	3.8 d	β^- (92) EC (8)	0.139	9	1.075	0.323	3.6	1.8

Re-188 與 Re186 射源之使用各有其優缺點， 以我們在台灣使用與發展上，Re-188 可自鎢-188 發生器獲得，而 Re-186 必須每次向國外購買，因此在射源使用與取得 Re-188 較具優勢；然而 Re-188 β-ray 平均能量 765 keV，平均穿透組織射程爲 3.5 mm，比起 Re-186 β-ray 平均能量 323 keV，平均穿透組織射程爲 1.8 mm，對小腫瘤而言，配合藥物傳輸系統研發，若 Re-186 能特異(specific)送到腫瘤部位，對周圍的正常的細胞傷害較小。然而在使用 Re-188/ Re-186 射源做爲治療性核醫藥物，都必須注意腸道細胞對輻射線之影響。

核研所正發展 Re-188-Liposome Doxorubicin (Re-Lipo-DOX)作爲大腸直腸癌之組合性放射與化療藥物，並應用於小鼠腫瘤與腹水模式之治療，並進一步建立輻射劑量評估，分析藥物在正常器官與腫瘤之輻射劑量。本次會議發表之研究成果爲注射 Re-188-Liposome 放射微脂體藥物及 Re-188-DOX-Liposome 放射化療微脂體藥物後，模擬 70 公斤成人，經輻射劑量評估，皆能預估正常組織接受的輻射劑量(mGy/MBq)，並估算最大容許注射劑量。其結果並接獲 Cancer Biotherapy and Radiopharmaceuticals 期刊

通知接受刊登，對核研所輻射劑量評估之建立與應用有很大助益。

目前德州大學臨床前試驗是使用人類卵巢癌或頭頸癌大鼠的裸鼠動物模式，初步的研究進度已完成，並證明放射性同位素標幟微脂體(Re-186-liposome)能夠有效的抑制腫瘤，同時亦已完成輻射劑量評估，在 Re-186-BMEDA-liposome 之大鼠造影研究中，可見腹腔注射後之不同時間造影結果，證明 Re-186-BMEDA-liposome 能有效滯留於體內。目前德州大學正在進行臨床試驗申請之準備，包含射源，相關藥品標幟方法，動物實驗數據，輻射劑量評估數據等文件整理，同時亦希望朝符合 GLP 規範而努力，目前美國並無針對治療核醫藥物的臨床前 CRO 公司，因此大部分實驗室在學校醫院或藥廠執行。

職與 Goins 教授教授進一步討論後續進展，他非常大方與熱心的說明臨床試驗之規劃與進展，他們亦瞭解臨床上市的困難，所以德州大學先進行臨床前動物模式研究，之後再進行一至二年之臨床試驗；Re-186-BMEDA-liposome 在進行人類卵巢癌或頭頸癌的大鼠裸鼠動物模式治療試驗時，最重要的是建立療效評估方式，他們亦建立活體分子影像分析技術，利用 FDG-microPET 進行腹腔腫瘤之生長分析，然後再進行後續的 FDG-microPET 療效評估分析，由於腹腔亦有 FDG 之非特異性吸收，所以使用大鼠模式較好，他們建議我們亦可使用大鼠模式以避免腹腔之干擾，只是國內尚未引進大鼠之裸鼠動物模式。

本次年會中有關蛙皮素(BBN)之研發可了解，近年來許多研究利用放射性同位素(Lu-177, In-111, Tc-99m, Re-188)標幟蛙皮素衍生物，藉由標幟的胃泌素衍生物對其受體的專一性結合，藉此找出腫瘤的位置，進行造影診斷或腫瘤放射治療之用。美國 Bracco 藥廠利用 Lu-177 標幟 BBN 衍生物進行攝護腺癌研究，目前已在歐洲進行臨床試驗，在 2012 年美國市場預計有一億兩千萬美金之市場，因此從國際會議與市場潮流而言，發展 Bombesin 爲放射治療之重要方向之一。

螢光/冷光活體動物體內成像系統具有非放射性、操作成本低之特性，然而螢光/冷光試劑之光學穿透性差，使其僅限至於小鼠及基礎研究，無法進一步應用於臨床研究；

而單獨放射性核醫造影具有光子穿透性佳，造影可由小鼠應用至人體，其臨床前研究成果可進一步應用於臨床研究，然而操作成本高及使用放射性物質爲其相對之缺點；因此由華盛頓大學利用 ^{177}Lu-LS308 (RGDfk) peptide-DTPA 及遠紅外光染劑進行放射治療，並利用不同的造影系統來追蹤療效評估之經驗得知，結合螢光/冷光活體動物體內成像系統、MRI、CT 與核醫分子影像之研究，這將是未來分子影像技術應用於生物醫學研究之重要方向。

在核醫分子影像技術方面，除繼續研發偵測晶體以增加敏感度與解析度外，目前亦朝向以研發影像重建技術與影像融合而努力；核醫分子影像目前主要爲多功能影像 microPET/CT, microSPECT/CT, microPET/microSPECT/CT 及 microPET/MRI 之影像融合，配合疾病機制爲研究主流，然而近兩年已有結合 microPET 與非放射性活體動物體內成像系統 (Bio-luminescence and Fluorescence, In vivo optical Imaging system)之研究，在本次會議其非放射性活體動物體內成像系統之研發報導與其核醫分子影像融合亦占許多比例，此亦是分子影像之重要一環。本會議中亦有許多研究使用非放射性活體成像 (Bio-luminescence and Fluorescence, In vivo optical Imaging) 來觀察實驗動物體內生物反應，即時追蹤微脂體在生物體內的分佈與活性，透過活體動物體內成像，可以觀測到疾病或癌症的發展進程以及藥物治療所產生的反應；活體成像系統的優點有：高敏感性、可進行連續、實時監測、相對於核醫影像系統之操作成本，其價格相對較低。

此外，磁振造影(Magnetic Resonance Imaging, MRI)不具侵襲性，也不會產生游離輻射，將放射診斷醫學帶入了另一個嶄新的領域。與斷層掃描相比，MRI 之成像原理，是依據核磁共振之基本原理，利用外界儀器改變體內氫原子的旋轉排列方向，此時原子核會釋放吸收的能量，能量激發後會放出電磁波信號，再經由電腦分析組合成影像，就是一般看到的MRI 影像。因此，MRI 具有高組織分辨力、空間分辨力、無硬性僞訊號及游離輻射之優點；同時於使用不同之顯影劑狀況下，可測量血管及心臟之血流變化、辨別腫瘤與周圍正常組織。由於MRI 乃基於組織器官型態改變作爲主要的影像診斷依據，而MRI 顯影劑的使用可加強型態改變之對比訊號強度，可於組織病變之早期即時發現，增加疾病早期治療的效果。因此MRI 技術之發展，除了掃描儀器設備之改善進

步外，另一個重要發展方向即爲顯影劑之開發。目前最常被使用的低磁化率(magnetic susceptibility)之順磁性顯影劑爲含釓(gadolinium) 有機金屬化合物，如Gd-DTPA及Gd-BOPTA (MultiHance)，MultiHance應用於肝臟及脾臟造影，經靜脈注射後，可快速分布至細胞外液，代謝途徑主要是原型藥品直接由腎小球濾出，最後再經由尿液排出。

2008 年會議中量子點(quantum dot)亦有許多探討，量子點是準零維(quasi-zero-dimensional)的奈米材料，由少量的原子所構成。粗略地說，量子點三個維度(x, y, z)的尺寸都在 100 奈米(nm)以下，外觀恰似一極小的點狀物，其內部電子在各方向上的運動都受到侷限，所以量子侷限效應(quantum confinement effect)特別顯著。由於量子侷限效應會導致類似原子的不連續電子能階結構，因此量子點又被稱爲「人造原子」(artificial atom)。科學家已經發明許多不同的方法來製造量子點，並預期這種奈米材料在二十一世紀的奈米電子學(nanoelectronics)上有極大的應用潛力。量子點的用途相當廣泛，在醫療上更利用各種發光波長不同的量子點製成螢光標籤，成爲生物檢測用的「奈米條碼」，這是創新的奈米科技，新一代的螢光試劑，因爲光譜的專一性以及螢光強度極爲鮮明亮麗而不會衰減，所以，已應用於許多生物醫學之研究。

Biomarker Imaging 在新藥開發過程扮演愈來愈重要的角色，在疾病或腫瘤發生過程中，腫瘤細胞會表現出特別的 Biomarker，利用 Biomarker 造影劑除可追蹤腫瘤生長外，最重要的是可以早期分析新藥的療效評估，目前常用的 Imaging Biomarker 爲 F-18-FDG, F-18-FLT, F-18-FMAU 等；利用這些能呈現生理代謝情形的 Biomarker 造影劑，配合分子影像設施，將能提早了解藥物之作用，已決定是否進行後續臨床試驗，或於臨床試驗進行中決定是否繼續後續的試驗，此一方式能夠節省大量新藥開發的成本與時間。

轉譯研究(Translational Research)近年來已成爲加速醫學研究的動力之一，轉譯研究就是將基礎研究的成果，經由科學實驗證實之後，轉譯成臨床的應用；而醫學研究的本質是創新，任何研發進展都必需經由許多研究人員不斷奉獻與付出，而最重要的是這些醫學研究之成果能經由臨床轉譯研究落實，並應用於協助解決患者之病痛，以達到促進

全民健康之最終目的。目前由於轉譯醫學、細胞生物學、分子生物學與分子影像科技之蓬勃發展，預計在 2020 年配合 MRI/PET 造影，加上個人化的解剖、細胞生理與分子遺傳資訊，將能達到個人化醫學，依個人的條件給予適當的治療。

四、建議事項

1. 核研所之研究能力已受國際研究單位與學者注意，應把握機會集中部份研究主題與國際合作，共同發表學術論文，以提高研究能力與知名度，就長遠規劃而言，即能朝共同發表專利，研發成果進行臨床試驗與醫藥品上市為目標而努力。

2. 核研所就分子影像之核心設備而言，跟得上國際趨勢，配合核醫與活體分子影像，核研所在腫瘤分子影像方面具有獨特性。惟分子影像方面之放射化學、藥物標幟與放射藥理之人才仍嫌不足，本所仍應加強人才培訓，建議未來能派員至國外著名單位實習，或在國內進修研究工作領域之博士學位，帶入新技術與知識，掌握最新研發趨勢與應用情形，將有助於核研所在分子影像領域之發展。

3. 核研所皆有一系列完整的設備及研究人員，在國內外，在轉譯醫學與分子影像應用於診斷與治療藥物開發都極具競爭力，核研所除集中核醫分子影像之專業，保有本身的優勢外，亦須進一步成立核醫藥物轉譯中心與 GLP 放射毒理實驗室，加速新藥開發時程。

4. 建議未來能持續派有經驗之研究人員參加此類國際分子影像研討會，發表論文，必與國外學者面對面討論，以吸收新技術，將有助於核研所在腫瘤與腦神經分子影像領域之發展及建立與國際研究單位合作之管道。

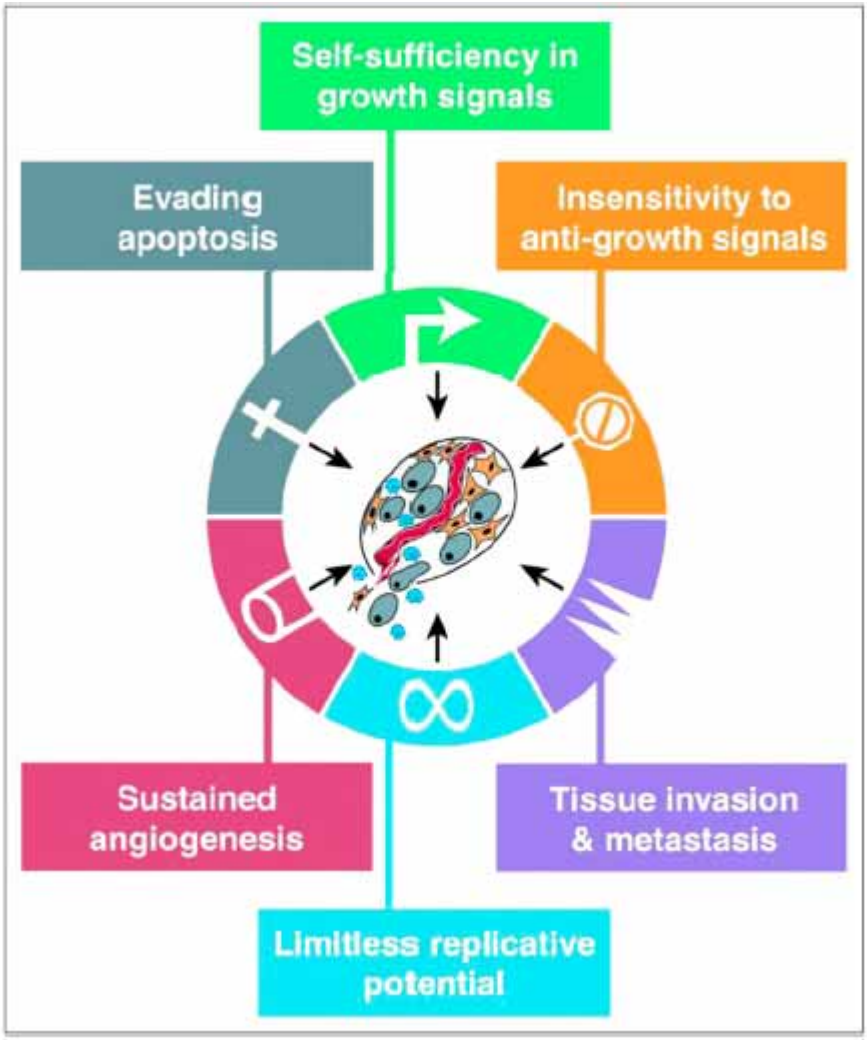

圖一 腫瘤細胞爲了生長與轉移而具有許多生理特徵。

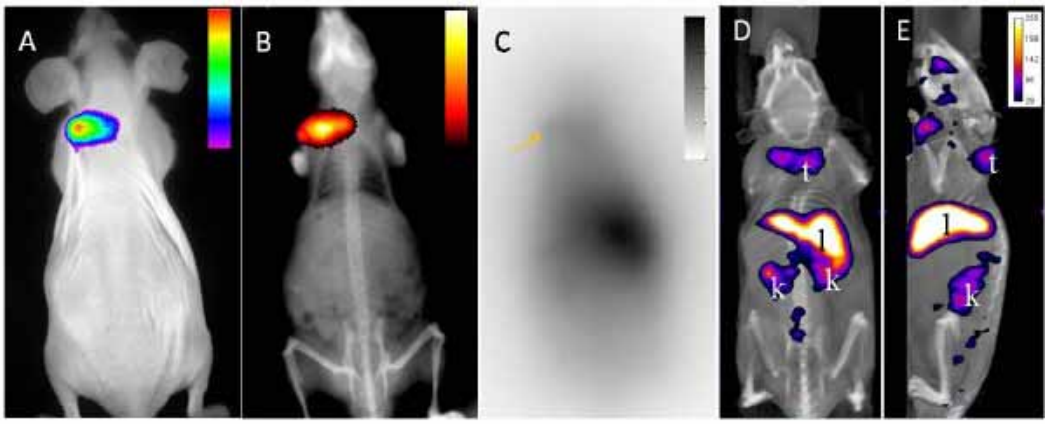

圖二 Multimodality Molecular Imaging 之應用，華盛頓大學利用 ^{177}Lu-LS308 (RGDfk) peptide-DTPA 及遠紅外光染劑進行放射治療，並利用不同的造影系統來追蹤療效評估之結果。(A)遠紅外光染劑造影；(B)冷光造影；(C)Gamma camera 平面造影；(D)microSPECT saggital view；(E)microSPECT coronal view。

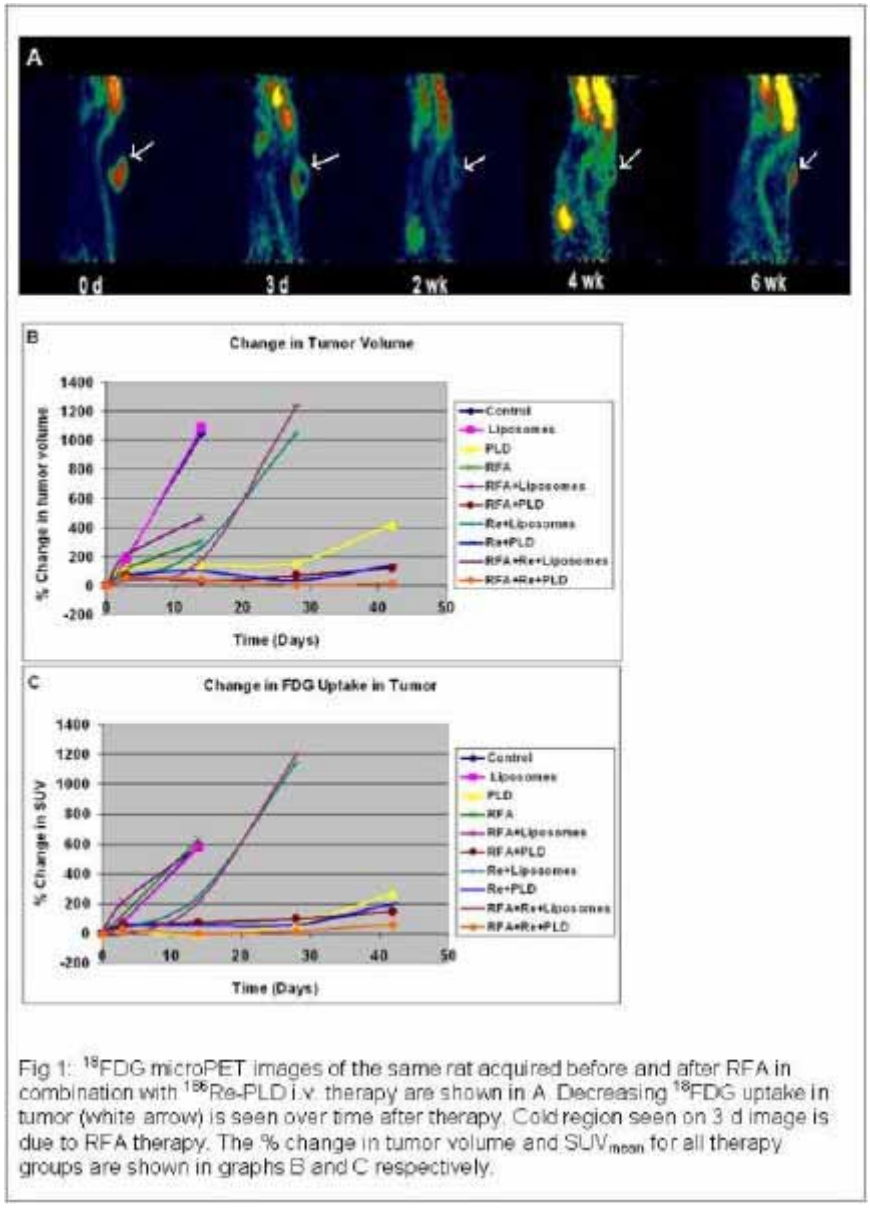

Fig 1: ^{18}FDG microPET images of the same rat acquired before and after RFA in combination with ^{186}Re-PLD i.v. therapy are shown in A. Decreasing ^{18}FDG uptake in tumor (white arrow) is seen over time after therapy. Cold region seen on 3 d image is due to RFA therapy. The % change in tumor volume and SUV_{mean} for all therapy groups are shown in graphs B and C respectively.

圖 三 德州大學聖安東尼奧校區發表 Re-186-PEG-liposomal doxorubicin (PLD)研究成果，他們使用頭頸癌的大鼠的裸鼠動物模式，證明放療加化療的治療結果最好。

圖 四 飛利浦公司近年成立轉譯影像中心，以縮短新藥研發至臨床上市的時間。

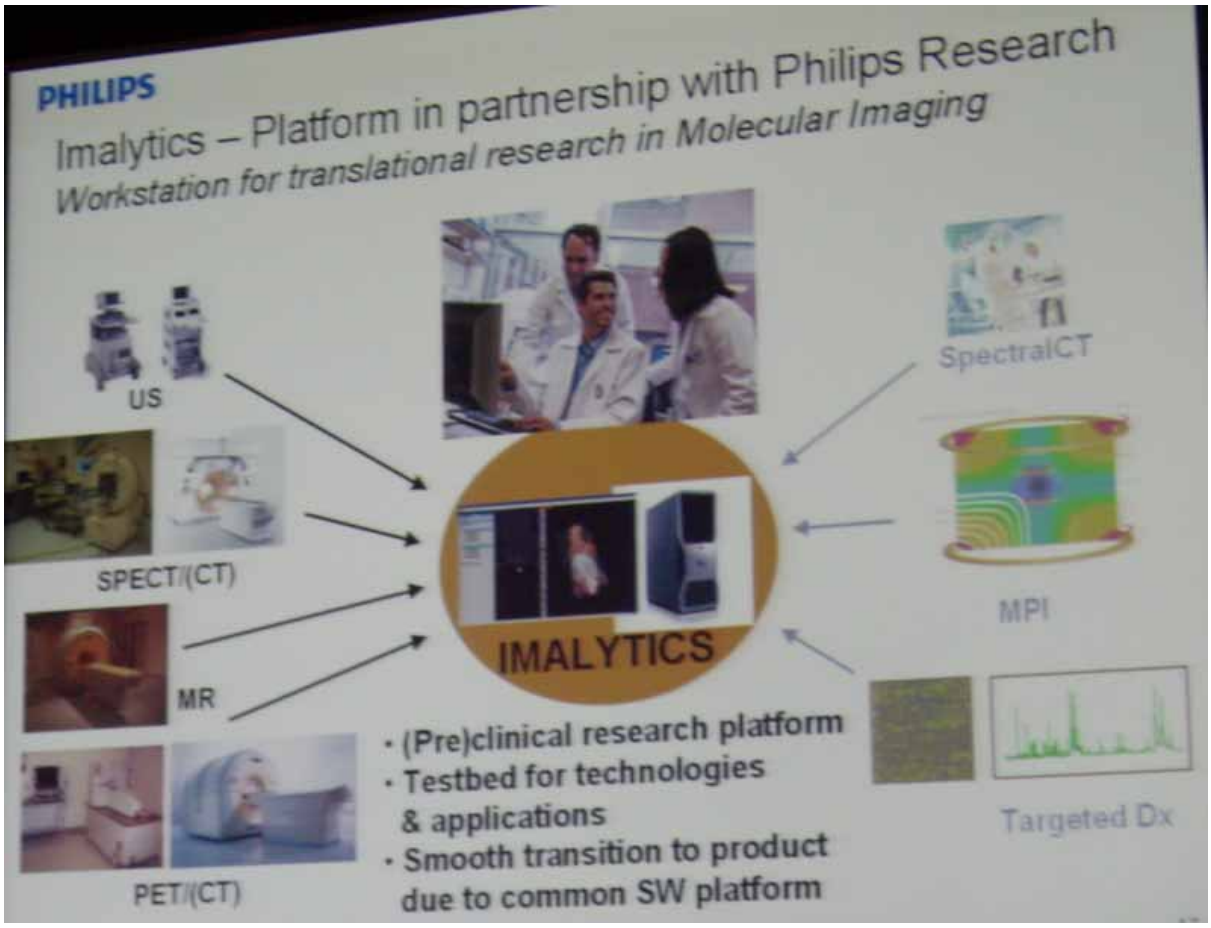

圖 五 飛利浦公司轉譯影像中心，臨床前與臨床研究技術平台。

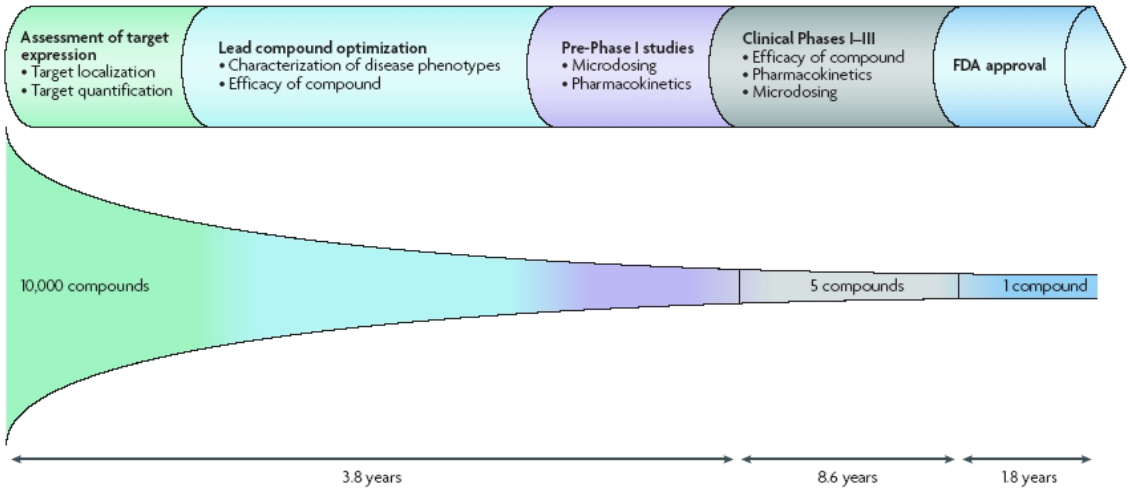

圖 六 藥物開發流程與時程。

Table 2 | **Therapeutic radionuclides**

Radionuclide	Type	Half-life	E_{max} (MeV)	Mean range (mm)	Imageable
^{90}Y	β	2.7 d	2.3	2.76	No
^{131}I	β, γ	8.0 d	0.81	0.40	Yes
^{177}Lu	β, γ	6.7 d	0.50	0.28	Yes
^{153}Sm	β, γ	2.0 d	0.80	0.53	Yes
^{186}Re	β, γ	3.8 d	1.1	0.92	Yes
^{188}Re	β, γ	17.0 h	2.1	2.43	Yes
^{67}Cu	β, γ	2.6 d	0.57	0.6	Yes

圖 七 治療腫瘤放射性同位素，它們的物理性質。

附錄

會議議程

DAY 0 September 10

12:00-17:00	REGISTRATION in "AGORA"
17:00-17:30	OPENING CEREMONY
17:30-18:15	INAUGURAL LECTURE by Markus Schwaiger: "Advances in Molecular Imaging from Bench to Bedside"
18:15-19:45	OPENING RECEPTION on the "RHODES Exhibit Hall"

DAY 1 September 11

	Educational Session 1 Quantitative In Vivo Pharmacological Imaging Co-Chairs: Richard Carson and Gitte Knudsen	Educational Session 2 Cell Labeling Methodologies Co-Chairs: Win-Ping Deng and Joseph Frank	Educational Session 3 In Vitro Molecular Imaging Assays Co-Chairs: Clemens Lowik and David Piwnica-Worms	Educational Session 4 Discovery of New Imaging Targets Co-Chairs: Christopher Morris and Renata Pasqualini	Educational Session 5 Reporter Genes Co-Chairs: Vikas Kundra and Andreas Jacobs
7:00-7:30	Compartmental Modeling AA Lammertsma	Molecular-genetic reporter labeling of stem cells for imaging Win-Pin Deng	Optical in vitro molecular imaging assays David Piwnica-Worms	In vivo Phage Display methods for discovery of new targets and imaging ligands Wadih Arap	Introduction and Clinical Translation of Reporter Gene Imaging Vikas Kundra
7:30-8:00	Parametric Receptor Imaging Richard Carson	Magnetic labeling of stem cells and immune cells for imaging Ali S Arbab	In vitro radiotracer kinetics assays: methods and measures Juri Gelovani	Identification of Neuroimaging Targets in Dementia Using Whole Genome Approaches Chris Morris	Applications of Reporter Gene Imaging in Neuroscience Alexandra Winkeler
8:00-8:30	In vivo Pharmacology. Gitte Knudsen	Labeling of stem cells and immune cells for optical imaging Vladimir Ponomarev	Reference molecular-biological assays for validation of novel molecular imaging agents Anna Planas	Target selection and effective probe development Julie Sutcliffe	Molecular Basis of Imaging Gene Expression Philip Liu
8:30-9:00	Coffee break				
9:00-9:45	Plenary Lecture 1	Advances in Stem Cell Biology and Imaging, Bernd Fleischmann			
9:45-10:30	Coffee break				
	Scientific Session 1 Molecular Imaging of Stem Cells Co-Chairs: Win-Pin Deng and Joseph Frank	Scientific Session 2 Molecular Imaging of Vascular Targets Co-Chairs: Clemens Lowik and Renata Pasqualini	Scientific Session 3 Molecular Imaging of Gene Delivery and Expression Co-Chairs: June-Key Chung and Bertrand Tavitian	Scientific Session 4 Advances in Optoacoustic Instrumentation and Applications Co-Chairs: Paul Beard and Alexander Oraevsky	Scientific Session 5 SNIDD Molecular Imaging in Drug Development Co-Chairs: Michael Tweedle and Jean-Luc Vanderheyden
10:30-10:45	Doublecortin Promoter-Based Reporter Systems for Optical Imaging of Neurogenesis Couillard-Despres S	Therapeutic Implications of Vascular Trgeting and Nanotechnology Pasqualini, R	Molecular Imaging of Gene Delivery and Expression Andreas Jacobs	Probing microvascular morphology, blood oxygenation and gene expression with in vivo functional and molecular optoacoustic imaging: current progress and future prospects Zemp R	Use of Exploratory INDs for Selection of 18F-AV-45 as a PET Amyloid Plaque Imaging Agent Daniel Skovronsky

10:45-11:00	Combined Real-time Bioluminescence and Magnetic Resonance Imaging to Monitor Mesenchymal Stem Cell Implantation in the Central Nervous System of Mice De Vocht N	Molecular Imaging of Vascularisation and Function using BLI Clemens Lowik	Novel Viral Vectors for Multi-Modality Imaging of Tumor-Targeted Gene Delivery and Expression Krasnykh V	A High Resolution Optoacoustic Scanner Based on an Optical Ultrasound Sensor for Imaging of small animals Beard P	Use of exploratory IND for Early phase clinical trials using PET or SPECT Imaging Gilles Tamagnan
11:00-11:15	Repetitive [18F]FEAU PETICT imaging for Monitoring the Migration and Engraftment of an sr39HSV1-tk Reporter Gene-Expressing Mesenchymal Stem Cell (MSC) after NOGAassisted Transendocardial Implantation in a Porcine Model of Acute Myocardial Infarction Marini F	Phage display selected peptide identifies furin protease as potential target for imaging target on pediatric soft tissue sarcoma rhabdomyosarcoma Bernasconi M	PET Assessment of Transgene-Mediated Dopamine Synthesis in a Primate Model of Parkinson's Disease S-IMuramatsu	Photoacoustic CT Scanner for Preclinical Molecular Imaging Kruger R	Radioligand discovery during Hit-to-Lead in CNS Drug Development: Earlier can be Better Mark Schmidt
11:15-11:30	Non-Invasive Imaging of Gene Expression in Implanted Human Mesenchymal Stem Cells in the Porcine Heart: A Further Step Towards Clinical Translation Willmann J	Conjugated Branched Peptides as Targeting Agents for Tumor Imaging and Therapy Pileri S	Imaging siRNA silencing in vivo with a ribozyme-mediated reporter So M-K	Photoacoustic Molecular Imaging with simultaneous intravascular and extravascular targeting Pai Chi LI	Detection of Dose Response in Chronic Doxorubicin mediated Cell Death with Cardiac SPECT 99mTc Annexin V Imaging Kathleen Gabrielson
11:30-11:45	Prevention of Osteoporosis in SAMP8 Mice by Growth Factor Extract and Progenitor Cell-Based Transplant Wu A	MicroCT Imaging of Angiogenesis in Non-Small Cell Lung Cancer (NSCLC) by Tumor Vasculature Targeting Dunne M	A Titratable Two-Step Tran-scriptional Amplification Strategy for Cardiac Gene Therapy Based on Ligand-Induced Intramolecular Folding of a Mutant Estrogen Receptor Chen I	In vivo whole body fluorescent protein imaging by means of multispectral optoacoustic tomography Daniel Razansky	Recombinant Escherirchia Coli and Attenuated Salmonella Typhimurium As a Tumor Targeting Imageable Thera-peutic Probe Jung-Joon Min
11:45-12:00	Quantitation of Iron Oxide Nanoparticles, BrdU and GFP uptake by Local Tissue Macrophages from Labeled Bone Marrow Stromal Cells Implications for Cellular Imaging Pawelczyk E	Molecular Imaging of Atherosclerosis using PEG-Micelles targeted by an ApoE Derived Peptide Vucic E	Gene-Based Contrast for MRI: Comparison of MagA and Modified Ferritin Subunits Goldhawk D	High Sensitivity Optoacoustic Molecular Imaging using Single Walled Carbon Nanotubes in Living Mice De la Zerda A	A novel nanomedicine-based anti-inflammatory treatment for atherosclerosis monitored by clinical multimodality imaging Willem Mulder
12:00-13:00	Lunch Break				
	Scientific Session 6 Molecular Imaging of Immune Cell Therapies Co-Chairs: Vladimir Ponomarev and Mathias Hoehn	Scientific Session 7 Molecular Imaging in Radiobiology and Radiotherapy Co-Chairs: Ted Graves and Andreas Brahme	Scientific Session 8 Molecular Imaging of Infection Co-Chairs: Christopher Contag and Martin Pomper	Scientific Session 9 Advances in Optical Instrumentation Co-Chairs: Vasilis Ntziachristos and Elizabeth Hillmann	Scientific Session 10 Molecular Imaging of Antibody Therapies Co-Chairs: Ana Wu and Vladimir Tolmachev
13:00-13:15	Nuclear Imaging in Cancer Immunotherapies Vladimir Ponomarev	PET-CT, Dose and dose response Imaging in photon and light ion therapy Andres Brahme	Molecular Imaging of Infection - State of the Art Oyen WJ G	Advances in Photonic Imaging Vasilis Ntziachristos	Advances in Molecular Imaging with Antibodies Anna Wu
13:15-13:30	A Critical Re-Examination of the Capability of MRI to Detect Macrophage Infiltration into Ischemic Tissue Tracy Farr	In Vitro Optical Imaging of Host Organ-Specific Tumor Responses to Radiation Schwartz D	Molecular Imaging Strategies for Tuberculosis: Visualizing the White Plague Cirillo J	Simultaneous PET and Multispectral Three-Dimensional Fluorescence Optical Tomography Imaging System forSmall Animals Cherry, S	Affibody molecules - high affinity scaffold proteins Vladimir Tolmachev

13:30-13:45	Optical Imaging in the Pre-Clinical Development of Cancer Immunotherapies Steven Thorne	Effects of Radiation on NF-κB and Hypoxia in Breast Xenograft Model Stantz K	Real time non-invasive assessment of inflammation and bacterial load in live TB-infected animals Jain S	Hybrid X-ray CT / FMT approach for high-performance molecular imaging applications Schulz, R	Antibody PET Imaging in Cancer Detection and Treatment Steven Larson
13:45-14:00	Tracking of Dendritic Cells in Melanoma Patients Jolanda de Vries	Correlation between various molecular imaging based dose painting targets in radiation oncology Jeraj R	Manifestation of Extrapulmonary Tuberculosis Infection on Integrated Fusion Imaging Modality Positron Emission Tomography Computed Tomography ; A Pilot Study Nordin A	Pump-Probe Optical Coherence Tomography Development for High-Resolution Imaging of the Microvasculature Applegate B	Immuno-PET: a navigator in monoclonal antibody development and clinical applications Guus van Dongen
14:00-14:15	Cellular MRI of Magneto-vaccination and DC Homing to Lymph Nodes as a Surrogate Marker of In Vivo T Cell Activation Long C	Optimizing PET-CT quantification for radiation treatment planning in treating cancers of the head and neck Hadi M	Image-guided gene expression profiles of the pathogen Listeria monocytogenes in vivo Elmerman P	Spatially-Modulated Near-Infrared Imaging for Image-Guided Surgery Gioux S	Overview of Pretargeted Immuno-SPECT and Immuno-PET Goldenberg D
14:15-14:30	Preclinical molecular imaging and monitoring of causative T-cells during Graft Versus Host Disease Formation and during Anti-GVHD Treatment using repetitive [18F] FEAU PET Imaging Marini F	Combined Parametric Response Mapping (PRM) of Diffusion and Perfusion Changes During Radiotherapy Enhances Survival Prediction in High Grade Glioma Hamstra D	Imaging EBV and KSHV-associated tumors in Vivo Fu D-X	Real-time multi-spectral surgical fluorescence imaging using attenuation correction Themelis G	Assessment of Structure-Biodistribution Relationship for Optimal Nanobody Design for in vivo Imaging Vaneycken I
14:30-15:15	Coffee break				
15:15-16:00	Plenary Lecture 2	Advances in Imaging Adoptive Cell Immunotherapies Caius Radu			
16:00-17:00	Poster Session, Coffee				
17:10-18:40	Workshop 1 Optical Imaging: From Chemistry to Clinical Translation (GE Healthcare)	Workshop 2 Fluorescence in vivo Imaging: Translational Data from Research through Medicine (VisEn Medical)	Workshop 3 Revolutions in Pre-clinical Imaging (GE Healthcare)	Workshop 4 Advancing Translational Medicine: Illustrations with Molecular Imaging (Philips)	Workshop 5 Developing Imaging Radiopharmaceuticals for the Future (IBA Molecular) Calliope Room
18:40-20:00	Free Time				
20:00-11:00	Evening and Cultural Events				

DAY 2 September 12

	Educational Session 6 Combined MRI/PET Technology Co-Chairs: John Clark and Simon Cherry	Educational Session 7 Reporter Animals as Novel Tools for Drug Discovery Co-Chairs: Sam Gambhir and Adriana Maggi	Educational Session 8 Radiopharmaceuticals for Molecular CNS Imaging Co-Chairs: Denis Guilloteau and Christer Halldin	Educational Session 9 Approaches to Nanoparticle Development Co-Chairs: Chun Li and Luisa Decola	Educational Session 10 Molecular MRI of CNS Imaging Co-Chairs: (EIBIR) Mathias Hoehn and Mike Modo
7:00-7:30	Introduction to PET/MRI, Simon Cherry	Designing Reporter Mice Christopher Contag	Regulation Issues for Radioligand development for Molecular CNS Imaging Alfons Verbruggen	Core-Shell Structured Metal Nanoparticles in Cancer Diagnosis and Therapy, Chun Li	Issues of fMRI in Rodents Mathias Hoehn

7:30-8:00	Different Approaches to Achieving Integrated PET/MRI Systems Rob Hawkes	Reporter Systems and Drug Development Adriana Maggi	Radioligand Precilnical evaluation for Molecular CNS Imaging Sylvie Chalon	Multi-modality Nanoparticles Jeff Bulte	Brain Regeneration followed with MR Cell Tracking Mike Modo
8:00-8:30	Roadmap of first in vivo results on preclinical and clinical PET/MRI Bernd Pichler	Reporter Mice in Drug Development Peter Lassotta	Clinical PET Neuroscoence and Drug Development Christer Halldin	Nanoparticles and Nano-containers: Synthesis and Applications Luisa Decola	Axonal Tracing Using Manganese MRI Rick Dijkhuizen
8:30-9:00	Coffee break				
9:00-9:45	Plenary Lecture 3	Deep cancer invasion and resistance niches detected by infrared-excited two-photon microscopy, Peter Friedl			
9:45-10:30	Coffee break				
	Scientific Session 11 Molecular Imaging of Hypoxia Co-Chairs: Yasuhisa Fujibayashi and Bernd Pichler	Scientific Session 12 Molecular Neuro-Imaging Co-Chairs: James Frost and Andreas Jacobs	Scientific Session 13 Advances in PET and SPECT Instrumentation Co-Chairs: Simon Cherry and Steve Meikle	Scientific Session 14 Molecular Imaging for Detection and Characterization of Cancer with PET Co-Chairs: Juri Gelovani and Stefano Fanti	Scientific Session 15 Advances in Nanoparticle Imaging Approaches Co-Chairs: Sam Gambhir and Benoit Dubertret
10:30-10:45	Combined MRSI, Optical, and Mass Spectrometric Imaging Revealed Distinct Molecular Profiles in Hypoxic Breast Tumor Regions Glunde K	Molecular and Biomarker Imaging in Addiction and Dependence: Drug Development to New Diagnostics James Frost	Recent Advances in PET and SPECT Instrumentation Cherry S & Meikle S	Detection and Characterization of Cancer with PET: European Perspective Stefano Fanti	Application of 111In-Labeled Micelles in Molecular Imaging of EGFR-Overexpressed Cancer Lee H
10:45-11:00	Molecular Imaging Assessment of the Impact of Intermittent Hypoxia in Glioblastoma Multiforme Progression Hsieh C-H	Assessment of dopaminergic and opioidergic neurotransmission in addictive behaviour Mathias Schreckenberger	Time-of-flight Imaging Performance of a Lanthanum Bromide PET Scanner Karp J	Monitoring Response after Peptide Receptor Radionuclide Therapy (PRRT) in patients with metastacized neuroendocrine tumors (NET): Comparison of metabolic (F-18-FDG), molecular (Ga-68-DOTA-NOC) and morphologic response (RECIST) using PET/CT Richard Baum	Multiplexed Imaging in Living Mice Using Non-Invasive Raman Spectroscopy in Conjunction with 10 Spectrally Unique Raman Nanoparticles Zavaleta C
11:00-11:15	Longitudinal evaluation of tissue hypoxia and glucose metabolism in different preclinical models of cancer Coradeschi E	Translational PET Imaging of the type 1 cannabinoid receptor Koen Van Laere	Performance Investigation of a Trimodal SPECT-CT-OT Small Animal Imaging Instrument Peter J	Molecular Imaging of Tumor Proliferation for Evaluating Response to Treatment Ken Herrmann	Nanocrystal core high-density lipoproteins: A multimodal molecular imaging contrast agent platform Cormode D
11:15-11:30	Multimodality approach in the study of angiogenesis: Magnetic Resonance, Positron Emission Tomography and micro-Synchrotron Computer Tomography Dominietto M	Developing vigabatrin for treating drug addiction: From bench top to bed side Stephen Dewey	Characterization of a Sub-Millimeter, High Contrast SPECT System for Multimodality SPECT/PET/CT Small Animal Imaging Tainter K	Detection of Prostate Cancer with PET Franca Chierichetti	Bioimaging of cancer theragnostics using nanoparticle-conjugated AS1411 nucleolin aptamer Ko H-Y

11:30-11:45	A Comparative Study between [18F]fluoro-azomycin-beta-deoxyriboside, [18F]fluoroazomycin-alpha-deoxyriboside, [18F]FAZA and [18F]FMISO Maier F	Imaging HIV-associated depression using [11C]DASB-PET Hammoud D	Latest Advances in Molecular Imaging Technology: PET/MRI Pichler B	PET/CT with 18F-Fluoroacetate and 18F-FDG, Serum and Tumor Tissue Biomarkers in Rhesus Macaques with Colon Carcinoma Tian M	Dual Modality Magnetic Resonance and Fluorescence Imaging Superparamagnetic Iron Oxide-Based Nanoprobe for Sentinal Node Imaging Bumb A
11:45-12:00	In Vivo Imaging of Tumor Oxygen Levels using Paramagnetic Resonance Imaging Matsumoto S	In Vivo PET Quantification of DA-Receptor and -Transporter Binding Potential in Mice Deficient of Large Conductance Calcium- and Voltage-Activated Potassium (BK) Channels Fischer K	Multi-functional PET/MR Imaging: First Results from Combined fMRI, ASL and PET Wehrl H	Molecular Imaging of EGFR Expression-Activity in Tumors with 18F / 124I -labeled oligoPEG-IPQA PET for Selection and Monitoring of Therapy Yeh, H-H	Theragnostics with Magnetic Gold Nanoshells: Photothermal Therapy and T2* Magnetic Resonance Imaging Melancon M
					#307 - 20; #235 - 20
12:00-13:00	Lunch Break				
	Scientific Session 16 Molecular Imaging of Inflammation Co-Chairs: Andreas Wunder and James Basilion	Scientific Session 17 Molecular Imaging of Neuro-Degenerative Diseases Co-Chairs: Karl Herholz and Chester Mathis	Scientific Session 18 Advances in MR Instrumentation Co-Chairs: Chrit Moonen and Tom Budinger	Scientific Session 19 Molecular Imaging of Cardio-Vascular System Co-Chairs: Markus Schwaiger and David Sosnovik	Scientific Session 20 Clinical Translation of Novel Oncologic Imaging Agents and Methods Co-Chairs: Johanes Czernin and Wolfgang Weber
13:00-13:15	Evaluation of [18F]PBR111 in a rat model of neuro-inflammation: a new radiotracer for the TSPO 18kD (Peripheral Benzodiazepine Receptor) Van Camp N	In vivo Imaging in Animal Models of Neurodegenerative Diseases: Where Are We Now? Doudet DJ	Biomedicine Horizons Resulting from Advances in Magnetic Resonance Instrumentation Budinger T	Advances MRI of Cardiovascular Diseases David Sosnovik	Radiation dosimetry and Biodistribution of 18F-HX4 Measured in Healthy Volunteers Yu, JQ
13:15-13:30	Tracking the Inflammatory Response in Stroke in vivo by Sensing the Enzyme Myeloperoxidase Breckwoldt M	Design, synthesis, and testing of difluoroboron derivated curcumins as "smart" near infrared probes for in vivo detection of amyloid-beta deposits Ran C	Multi-Channel RF-Coils for MRI of Small Animals in Clinical Environment Wichmann T	Molecular Imaging of Cardiovascular System Schafers, M	Pharmacokinetics, Biodistribution, Metabolism, and Radiation Dosimetry of [18F]FPEG6-IPQA in Non-Human Primates: A pre-IND Study Tian M
13:30-13:45	Live Imaging of TLR2 Induction and microglial activation in brain injuries Kriz J	Identifying Amyloid-Positive Controls using PIB PET Price J	Direct Imaging of Ferumoxides using Magnetic Particle Imaging: Instrument Con-struction, Sensitivity, and 3d Imaging Goodwill P	Optical Imaging in Cardiovascular Disease Kim, D	68Ga-DOTA-Tyr3-Octreotide PET in thyroid cancer patients compared to 18F-FDG-PET and radioiodine-avidity Putzer D
13:45-14:00	In vivo [18F]FAZA PET-Imaging of Inflammation-Induced Hypoxia in a Small Animal Model of Rheumatoid Arthritis Fuchs K	Association between microstructural and functional alterations in early AD: a combined DTI-PET study Yakushev	Local control of transgene expression using MRI guided HIFU on a transgenic mouse Deckers R	Fluorescence Reflectance Imaging of Macrophage-Associated Alpha(v)beta(3) Integrin Expression in Atherosclerotic Lesions with RGD-Cy 55 Waldeck J	Diffusion-Weighted MR Imaging (DWI) for Detection of Pelvic Lymph Node Metastases in Correlation with 11C-Choline-PET/CT - Preliminary Experience Eiber M

14:00-14:15	Molecular Imaging of VCAM-1 expression in inflammatory pathologies by using low molecular weight peptides conjugated to a paramagnetic reporter Burtea C	Correlation of Glucose Metabolism and Microglial Activation in Multiple System Atrophy - a PET study Gerhard A	1D and 2D Correlation MR Spectroscopy at 7T: A Feasibility Study on Human BoneMarrow and Soleus Muscle Mountford C	Modulation of atherosclerotic plaque and Matrix Metalloprotainase (MMP) activity by Minocycline: Evaluation by molecular imaging of MMP expression Ohshima S	Targeted biotherapies of cancer assisted by optical imaging Jean-Luc Coll
14:15-14:30	Design and characterization of new MR imaging agents sensitive to myeloperoxidase activity Rodriguez E	In vivo SPECT imaging of vesicular acetylcholine transporter using [123I]-IBVM in neurodegenerative diseases Mazere J		NonInvasive Characterization of Human Carotid Plaques by Imaging of αvβ3 Expression with [18F]Galacto-RGD PET/CT Beer A	Image Fusion to Guide Molecular Interventions Wood B
14:30-15:15	Coffee break				
15:15-16:00	Plenary Lecture 4: #1669 Imaging Metabolism Kevin Brindle (UK)				
16:00-17:00	Poster Session, Coffee				
17:10-18:40	Workshop 6 Shaping the Future of Clinical and Preclinical Imaging (Siemens Medical Solutions)	Workshop 7 Molecular MRI of the Cardiovascular System and Novel Techniques for Tissue-based Proteomics based on Maldi Imaging (Bruker)	Workshop 8 68Ga Labeled Radiotracers in Molecular Imaging (Eckert & Zeigler Radiopharma GmbH, GE Healthcare, and Molecular Insight Pharmaceuticals)	Workshop 9 Molecular Imaging Strategies for in vivo Studies: One Kinetic Step ahead with BioSpace Labs Solutions (BioSpace Labs)	Workshop 10 Advances and Applications in Small Animal Multispectral and Multimodal Optical Molecular Imaging (Carestream Molecular Imaging, formerly Kodak Molecular Imaging)
18:40-20:00	Free Time				
20:00-11:00	Evening and Cultural Events				

DAY 3 September 13

	Educational Session 11 Approaches and Methods in MRI Probe Design Co-Chairs: Silvio Aime and Klaas Nikolai	Educational Session 12 Molecular Imaging of the Vascular System Co-Chairs: Michael Schäfers and Mike McConnell	Educational Session 13 Advances in In Vivo Microscopy Co-Chairs: Chen Yuang Dong and Christopher Contag	Educational Session 14 Radio-labeled Peptides in Tumor Imaging and Therapy Co-Chairs: Helmuth Maecke and Uwe Haberkorn	Educational Session 15 Aptamer Imaging Chair: Bertrand Tavitian
7:00-7:30	Molecular MR Imaging Using Paramagnetic and Superpara-magnetic Contrast Agents Gustav Strijkers	Scintigraphic Imaging of Atherosclerosis Michael Schäfers MRI of Vascular Inflammation Mike McConnell Fluorescence Imaging of Vascular	Developing Intravital Multiphoton Microscopy for Biomedical Research Chen Yuang Dong	Target Definition and Development of Receptor Antagonists Jean-Claude Reubi	Aptamers for Molecular Imaging Bertrand Tavitian Radiolabeling of Oligonucleotides for PET Imaging Frederic Dolle
7:30-8:00	CEST and PARACEST Agents Enzo Terreno	Disease David Sosnovik Targeted microbubbles - molecular imaging agents for intravascular targets	Advances in Microendoscopy Jon Liu	Evaluation of Non-SST Receptor Molecules Marion deJong	Live-cell SELEX on Whole Living Cells Agnes Cibiel
8:00-8:30	Hyperpolarization approaches for molecular sensing Leif Schroeder	Alexander Klibanov	New Dyes and Probes for In Vivo Microscopy Sam Achilefu	Problems of peptide identification: the day after biopanning Uwe Haberkorn	Selection and Imaging of Tumor Targeting Aptamers Frederic Duconge
8:30-9:00	Coffee break				

9:00-9:45	Plenary Lecture 5: Of Mice and Man and Imaging Markus Rudin				
9:45-10:30	Coffee break				
	Scientific Session 21 (RSNA) Novel Imaging for Clinical Studies Co-Chairs: Gabriel Kerstin and Jan Grimm	Scientific Session 22 (ISMRM) Advances in MR Probes and Spectroscopic Imaging Co-Chairs: John Waterton and Alexei Bogdanov	Scientific Session 23 Molecular Imaging of Epigenetic Regulation of Gene Expression Co-Chairs: Juri Gelovani and Eric Hostetter	Scientific Session 24 Advances in PET/SPECT Probes Co-Chairs: William Eckelman and Eyal Mishani	Scientific Session 25 Molecular Imaging of Apoptosis Autophagy & Necrosis Co-Chairs: Kevin Brindle and Leonard Hofstra
10:30-10:45	Requirements for Imaging from a Molecular Oncologist's Point on View Walter Stadler	Advances in MR Probes and Spectroscopy Sarah Nelson	Imaging and Drug Targeting of Epigenetic Regulation Eric Hostetter	Indium-111 Labeled Conjugates of Naltrindole: Radioligands for SPECT Visualization of Delta Opioid Receptors Expressed by Small Cell Lung Cancers Lever J	Annexin A5; Imaging Biomarker for Cell Death Leonard Hofstra
10:45-11:00	Imaging Biomarkers Adrian Nunn	A novel technique for screening a library of CEST MRI McMahon M	Assessment of Dose-Dependent Inhibition of HDACs Activity in the Rat Brain Induced by Different HDAC Inhibitors Using In Vivo PET Imaging with 18FAHA Yeh H-H	A Library Approach: Synthesis of 11C-Carbonyl-Labelled Irreversible Binding EGFR Inhibitors as Potential Biomarkers for Tumours Using [11C]Carbon Monoxide Aberg O	Molecular MRI of Apoptosis in the Heart within Four Hours of Ischemia Reperfusion Injury Sosnovik D
11:00-11:15	MR Imaging in Clinical Trials Larry Schwartz	A high relaxivity Gd(III)DOTA-DSPE-based liposomal contrast agent for target-specific MRI Nicolay K	[18F]FAHA is a Useful PET Tracer for Determining Inhibition of Central Histone Deacetylase (HDAC) Activity in Rhesus Monkey Hostetler E	Radiopharmaceutical Strategies for the Imaging of Angiogenesis in Cancer Ilovich O	Imaging Acute Cardiac Cell Death using 99mTc-Duramycin Zhao M
11:15-11:30	PET Imaging in Clinical Trials Gustav von Schulthess	In Vivo Evaluation of Tissue Redox Status using Metabolically Responsive MRI Contrast Agents Krishna M	Biodistribution and Radiation Dosimetry of [18F]-FAHA in Non-human Primates: a Pre-IND Study Nishii R	A Submicrogram-Scale PET Imaging of Biomolecules: New Labeling of Lysines via 6pal-Azaelectrocyclization Tanaka K	Imaging Of Intracellular Caspase-3 To Visualize Apoptosis Hermann S
11:30-11:45	Clinical Optical Imaging Michael Selden	Monitoring Dynamic Calcium Homeostasis Alterations by Cardiac Manganese-Enhanced MRI (MEMRI) with T1 Mapping in a Murine Myocardial Infarction Model Waghorn B	Measurement of hTERT gene silencing induced by specific siRNA using NIS reporter gene Kim S	Silicon-Based One-Step Method for 18 F-Labeling of Peptides and A Theoretic Model for Predicting Hydrolytic Stability Mu L	In Vivo Imaging of HSP60 expression after arterial… Wick M
11:45-12:00	Panel Discussion	Towards the Multiple Detection of MRI Probes Terreno E	Combination Therapy and Non-invasive Imaging Using a Dual Therapeutic Vector Expressing MDR1 shRNA and Sodium Iodide Symporter (NIS) Cha K	18F-labeled aryltrifluoroborates - products of a one step aqueous labeling of biomolecules with 18F-fluoride upon reaction with aryiboronic acids Perrin D	Cell-Permeable 99mTc(CO3)-Labeled Fluorogenic Caspase Substrate for Dual Modality Detection of Apoptosis Li C
12:00-13:00	Lunch Break				
	Scientific Session 26 (SNM) Overcoming Challenges in Clinical Translation of Novel Radiotracers Co-Chairs: Homer Macapinlac and Henry Van Brocklin	Scientific Session 27 Advances in MR Spectroscopy using hyperpolarized agents Co-Chairs: Arend Heerschap and Sarah Nelson	Scientific Session 28 (FASMI) Co-Chairs: Yasuhisa Fujibayashi and Ren-Shyan Liu	Scientific Session 29 Advances in US probes Co-Chairs: Alex Klibanov and Michel Schneider	Scientific Session 30 Molecular Imaging of Signal Transduction & Protein-protein Interactions Co-Chairs: David Piwnica-Worms and Andreas Jacobs

13:00-13:15	Advocacy & Molecular Imaging - A Challenge for the Field Atcher R	In Vivo Hyperpolarized 13C MR Spectroscopic Imaging In a Rat Model of Brain Tumor Ilwoo Park	Sentinel Node Navigation Surgery In Lung Cancer Using A Novel Receptor Binding Agent (Tc-99m Neomannosyl human serum albumin 99m Tc-MSA): First clinical trial and ongoing study Kim S	Advances in Contrast Agents for Ultrasound Molecular and Cellular Imaging Alexander Klibanov	Quantification of dynamic protein complexes in real-time using Renilla luciferase-fragment complementation Stefan E
13:15-13:30	Regulatory challenges for clinical translation of novel radiotracers in North America Schwarz S	Temperature-Controlled Signal Amplification for Detection of Functionalized Xenon Biosensors Leif Schröder	Near-Infrared Fluorescent Imaging of Cathepsin-B Enzyme Activity Reflects Anti-Atherosclerotic Effects Of Statin Both In Mice And Humans Kim J-Y	Molecular ultrasound imaging of vascular markers of inflammation in rodents Bettinger T	Construction of Protein Fragment Complementation Using GFP-like fluorescent protein Dronpa Han YS
13:30-13:45	Regulatory challenges for clinical translation of novel radiotracers in Europe Verbruggen A	Tumor and metastatic cancer cells detection using targeted contrast agent in IMQC and hyperpolarized 3He experiments Rosa T Branca	Targeted Therapeutic Evaluation on Inhibition of Fatty Acid Synthase in a Human Prostate Carcinoma LNCaP/tk-luc Bearing Animal Model with Molecular Imaging Tai W-T	Clinical Applications of Kupffer Cell Targeted Imaging of the Liver Using a New Ultrasound Contrast Agent Perflubutane Microbubble Moriyasu T	GPI anchored avidin- a novel protein reporter for in vivo imaging Lehmann S
13:45-14:00	Regulatory challenges for clinical translation of novel radiotracers in Asia Fujibayashi Y	Hyperpolarized MR Spectroscopy: An In Vivo Marker of PDH Activity Marie A Schroeder	Non-invasive reporter gene imaging for determining the inhibition kinetics of tumorigenesis by actin depolymerizing factor (ADF)/cofilin Lee Y-J	Targeted versus Free Circulating Ultrasound Contrast Agents: Towards New Molecular Imaging Strategies van Wamel A	Non-invasive assessment of E2F-1 mediated tranecriptional regulation in vivo Montared P
14:00-14:15	Predictive PET Imaging for Nucleoside Analog Resistance in Cancer Laing R	Tissue-specific T2 of Hyperpolarized 13C Metabolites Yi-Fen Yen	Development of a radiolabeled peptide derivative targeting matrix metalloproteinase-2 for imaging tumors Hanaoka H	Dual-targeted Contrast Agent for Ultrasonic Assessment of Tumor Angiogenesis in Vivo Willmann J	A double transgenic rat for the in vivo imaging of human prolactin dual promoter gene expression Semprini S
14:15-14:30	Comparison of Bone Scintigraphy and Imaging of αvβ3 Expression with [18F]Galacto-RGD PET for Evaluation of Osseous Metastases in Prostate Cancer Patients Beer A	Hyperpolarized Carbon-Carbon Intermolecular Multiple Quantum Coherences Warren W	MRI Probe to detect enzyme activity using paramagnetic relaxation enhancement Mizukami S	Activatable Perfluorocarbon Ultrasound Probes for Cellular Imaging Matsuura N	Molecular Imaging Captures the Highs and Lows of Endogenous Cdc25A in Mice and MEFs Piwnica-Worms H
14:30-15:15	Coffee break				
15:15-16:00	Young Investigator Award Session				
16:00-17:00	Poster Session Coffee				
17:10-18:40	Workshop 11 Current GMP Lifecycle and its Implications in PET: Facilities Design Manufacturing and Documentation				
19:00-23:00	GALA Event and Closing Ceremony				

附錄

發表論文摘要

Comparative Dosimetry and micro-SPECT/CT imaging of Nanotargeted ^{188}Re-(DXR)-Liposome in a C26 colon carcinoma mouse model.

Chih-Hsien Chang[1], Michael G. Stabin[2], Ya-Jen Chang[1], Liang-Cheng Chen[1], Min-Hua Chen[3], Tsui-Jung Chang[1], Te-Wei Lee[1], and Gann Ting[3]. [1]Institute of Nuclear Energy Research, Taoyuan, Taiwan, R.O.C.; [2]Vanderbilt University, Nashville, Tennessee, USA; [3]National Health Research Institutes, Miaoli, Taiwan, R.O.C.

A dosimetric analysis and micro-SPECT/CT imaging were performed to evaluate nanoliposomes as carriers of radionuclides (^{188}Re-liposomes) and radio-chemotherapeutic drugs (^{188}Re-Doxorubicin (DXR)-liposomes) in internal radiotherapy for colon carcinoma, as evaluated in mice. **Methods:** Pharmacokinetic data for ^{188}Re-N, N-bis (2-mercaptoethyl)-N',N'-diethylethylenediamine (BMEDA), ^{188}Re-liposome and ^{188}Re-DXR-liposome were obtained for estimation of absorbed doses in tumors and normal organs. Two colon carcinoma mouse models were employed: subcutaneous growing solid tumor and malignant ascites pervading tumor models. Radiation dose estimates for normal tissues and tumors were calculated using the OLINDA/EXM program. An evaluation of a recommended maximum administered activity (MAA) for the nanotargeted drugs was also made. **Results:** The tumor target and localization of the passive nanoliposome delivery radiochemo-therapeutics was demonstrated by micro-SPECT/CT imaging in mice. Mean absorbed doses derived from ^{188}Re-liposome and ^{188}Re-DXR-liposome in normal tissues were generally similar to those from ^{188}Re-BMEDA in intraperitoneal (i.p.) and intravenous (i.v.) administarion. Tissue absorbed dose in liver was 0.24 to 0.40 and 0.17 to 0.26 (mGy/MBq), and in red marrow was 0.033 to 0.050 and 0.038 to 0.046 (mGy/MBq), respectively for ^{188}Re-liposome and ^{188}Re-DXR-liposome. Tumor absorbed doses for the nanotargeted ^{188}Re-liposome and ^{188}Re-DXR-liposome were higher than those of ^{188}Re-BMEDA for both routes of administration (4 to 26-fold). Dose to red marrow defined the recommended MAA. **Conclusion:** Our results suggest that radionuclide and chemoradio-therapeutics passive targeting delivery using nanoliposomes as carrier is feasible and promising in systemic-targeted radionuclide therapy.

Key words: dosimetry; doxorubicin; internal radiotherapy; micro-SPECT/CT, pegylated nano-liposomes; rhenium-188

Biological Evaluation and microSPECT/CT imaging of ^{111}In-DTPA-Bombesin in PC-3 bearing SCID mice

Chung-Li Ho, Chih-Hsien Chang, Wan-Chi Lee, Shu-Pei Chiu, Liang-Cheng Chen, Yu-Hsien Wu, Chung-Hsin Yeh, Wei-Chuan Hsu, Te-Wei Lee

Institute of Nuclear Energy Research, LongTan, Taiwan.

Purpose: Bombesin (BBN) is a 14 amino acid peptide with high affinity for the gastrin-releasing hormone receptor (GRPr). We synthesized DTPA-Q-K-Y-G-N-Q-W-A-V-G-H-L-M (DTPA-BBN), a 13 amino acids peptides chelated with diethylenetriaminepentaacetic acid (DTPA), and radiolabeled this BBN analog with $^{111}InCl_3$. Bioactivity of ^{111}In-DTPA-BBN was evaluated in PC-3 tumor-bearing SCID mice. **Methods:** A solid phase approach was used to synthesize DTPA-BBN. The affinity of DTPA-BBN to BBN type 2 receptor was determined by a competitive displacement cell-binding assay using ^{125}I-Tyr^4-BBN. The hot saturation was using ^{111}In-DTPA-BBN and PC-3 prostate cancer cells. The PC-3 tumor-bearing SCID mice were imaged by microSPECT/CT and sacrificed for biodistribution at 1, 4, 8, 24 and 48 hr after iv injection of ^{111}In-DTPA-BBN. **Results:** The purity of DTPA-BBN was greater than 95%. The labeling efficiency of ^{111}In-DTPA-Bombesin was 98.0 ± 0.43%. The IC_{50} and Ki of DTPA-BBN were 1.05 ± 0.46 nM and 0.83 ± 0.36 nM, respectively. The Kd and Bmax of ^{111}In-DTPA-BBN were 22.9 ± 6.81 nM and 880 ± 420 fmole/10^6 cells, respectively. In microSPECT/CT imaging, the PC-3 tumor became prominent at 8 –24 hours after injection. For the biodistribution, the higest uptake of DTPA-BBN in PC-3 tumor was 2.48 ± 0.48 %ID/g at 8 h after injection. **Conclusions:** Our result revealed ^{111}In-DTPA-BBN has high affinity with BBN type 2 receptor. The biodistribution and microSPECT/CT images demonstrated that ^{111}In-DTPA-BBN showed a good uptake in the GRPr-over expression PC-3 tumor-bearing SCID mice.

[DTPA^1(^{99m}Tc(CO)$_3$), Lys^3, Tyr^4]Bombesin Biodistribution and SPECT/CT Imaging in SCID Mice with/without Receptor Blockade

Pan-Fu Kao*, Chung-Li Ho, Chi-Hao K. Kao*, Wan-Chi Lee, Liang-Cheng Chen, Chung-Hsin Yeh, Yu-Hsien Wu, Meei-Ling Jan, Chih-Hsien Chang, Te-Wei Lee, Ying-Kai Fu.

***Buddhist Tzu Chi General Hospital, Xindian City, Taipei, and Institute of Nuclear Energy Research, Lung-Tan, Taiwan.**

[**Background/Purpose**] Bombesin is a neuropeptide which over expressed on variety of cancers. We had performed serial [DTPA^1(^{99m}Tc(CO)$_3$), Lys^3, Tyr^4]bombesin ([Tc-99m]BN) animal SPECT/CT in SCID mice model in the last year. In this study, the authors used both bombesin and non-bombesin receptor expression cancers in SCID mice model for [Tc-99m]BN biodistribution and image studies with/without unlabeled BN pretreatment. The

purpose of this study was to establish the biodistribution data for radiation dose estimation and to test the specific binding of [Tc-99m]BN. [**Method]** For SICD mice tumor model, 10^6 cell of bombensin receptor expression PC-3 tumor and 10^6 cell of non-bombensin receptor expression CC7T tumor were implanted in the right and left thigh of SCID mice, respectively. Four SCID mice were sacrificed respectively at 1, 2, 4, 7, and 24 hours after [Tc-99m]BN intravenous injection for whole body biodistribution study. Two mice were sacrificed for autoradiography at 18 hours after [Tc-99m]BN injection. There were 6 mice for pretreatment biodistribution study with unlabeled bombesin, 2 had serial SPECT/CT images upto 18 hours after [Tc-99m]BN injection and then sacrificed for whole body autoradiography, 4 were sacrificed at 7 hours after [Tc-99m]BN injection for biodistribution. **[Results]** As compared with the previous serial study, the pretreatment [Tc-99m]BN animal SPECT/CT imaging revealed significantly decreased PC-3 tumor uptake. The biodistribution study showed that the PC-3 tumor [Tc-99m]BN activities at 2 and 7 hours after injection were about 3.5 and 2.6 times of the activity in CC7T tumor respectively. After blockade, the PC-3 to CC7T ratio decreased to 1.5. The pretreatment autoradiography also revealed decreased [Tc-99m]BN binding to the PC-3 tumor. **[Conclusion]** This preliminary study demonstrated the specific binding of [Tc-99m]BN in pre-clinical evaluation by SCID with PC-3 tumor model. The pharmacokinetic study results could provide data for radiation dose estimation in the future.

Auto-Synthesis and Research Study in Alzheimer's disease with [^{18}F]-FDDNP

KW Chang, YH Tu, SH Lee, CC Chen, HJ Chen

Division of Isotope Application, Institute of Nuclear Energy Research Atomic Energy Council, Taiwan

Objective(s) Alzheimer's disease (AD) is one of the epidemic neurodegeneration disease in older. Senile plaques (SPs) and neurofibrillay tangles (NFTs) are hallmarks in AD. Fluorescent molecular imaging probe, [^{18}F]FDDNP (2-(1-{6-[(2-[^{18}F]fluoroethyl)(methyl)amino]-2-naphthyl}ethylidene)malononitrile), showed the superiority characteristics in binding with SPs and NFTs. In the article, we modified the protocol in auto-synthesizer and used the radiopharmaceutics in vitro, in vivo and ex vivo study with transgenic mice (Tg2576).Wished complete a platform in diagnosis of AD.

Material & Method(s) In-house-labeling [^{18}F]FDDNP by an auto-synthesizer. Partition coefficient was measure the ratio between the aqueous buffer (PBS) and organic buffer (octanol). In vitro, in vivo and ex vivo study used Tg2576 brain section for the assay. Competitive assay used radio-free pharmeuticals co-incubation with brain section.

Result(s) High quality of [^{18}F] FDDNP (Radiochemical purity >90%) was synthesized by auto-synthesis. Partition coefficient value was 1.93 ± 0.10, means lipophilic ability to penetrate the blood brain barrier (BBB). In vitro competitive assay showed that high selectivity and specificity in Tg2576 brain region (selectivity between hippocampus and frontal cortex were 2.10 ± 0.34 and 1.90 ± 0.17, respectively, specificity between hippocampus and frontal cortex were 4.62 ± 1.58 and 7.27 ± 5.53, respectively.) In vivo bio-distribution assay, control mice showed faster washout from brain at 30 min, in Tg2576 mice the accumulation is still sustainable in the brain. In ex vivo assay, whatever from 5 min to 60 min, Tg2576 mice brain accumulation is higher than control mice about 2 to 3 fold.

Conclusion(s) Auto-synthesizer had success applied the synthesis protocols in [^{18}F]FDDNP. In the report, we made the higher quality product and in those experiments were showed the superiority results. Our future plan were using transgenic mice in vivo imaging by microPET. Wish to exploitative the platform for diagnosis AD.

Evaluate the effect of X-911 on LL2 lung tumor bearing nude mice by small animal PET Imaging

Li-Chung Hwang、Jun-Ming Shih、Yu-Lung Wu、Chia-Chieh Chen、Haw-Jan Chen

Purpose:

The aim of this study was try to evaluate the effect of X-911, an herb extract sterols complex, on the LL2 tumor bearing nude mice animal model by small animal PET imaging.

Material and method:

Male nude mice (20-25 grams) were used in this study. Twenty LL2 tumor-bearing nude mice were set into four groups: control, high dosage (125mg/day), low dosage (62.5mg/day) and pre-treated (125mg/day). Pre-treated group was administrated 125mg of X-911 two weeks before LL2 lung tumor implanted. In high and low dosage groups, X-911 was given 5 days a week after 10 days tumor implanted. ^{18}F-FDG PET imaging was performed and tumor volumes were measured in each group.

Result:

^{18}F-FDG PET imaging showed tumor sizes in high dosage, low dosage and pre-treated groups were obviously diminished compared with control group at 28 days after tumor implanted. And above all, low dosage group had greatest tumor growth inhibition about 50% ($p < 0.05$) than high dosage (82%) and pre-treated (56%, $p < 0.05$). Tumor volume ratios (compared with control) in both high and low dosage group were reduced with time. However, it's slight increase in pre-treated group. At 35 days after tumor implanted, the tumor sizes in high and low dosage groups were further decreased to 80% and 47%, respectively but increased to 69% in pre-treated group.

Conclusion:

In conclusion, the tumor growth inhibitive ability of X-911 showed no dose-dependent manner. Pretreatment of X-911 could initially inhibit tumor growth but the effect would decay with time. The inhibition effect on tumor growth of X-911 was found to have the order of: low dosage > pre-treated > high dosage.

Tc-99m-ECD Brain Image on B6 Stroke Mice Animal Model by Small Animal Multi-pinhole SPECT

Jun-Ming Shih, Li-Chung Huang, Kuo-Hung-Wu, Hsiu-Ru Shen, Bi-Fang Lee, Chia-Chien Chen, Haw-Jan Chen

Purpose :

We used technetium-99m-ethylcysteinate dimer (Tc-99m -ECD) brain imaging to monitor blood flow in B6 stroke mice animal model by multi-pinhole SPECT. This study attempts to determine the usefulness of 99mTc-ECD SPECT in evaluating *in vivo* regional blood flow in cerebral infarct area on mice.

Material& method:

Male C57BL/6J mice (20-25 grams) were used in this study. Permanent focal ischemia was induced by occlusion of the right middle cerebral artery (MCA) in mice. We prepared Tc-99m -ECD using a two-vial kit, the concentration of radioactivity was about 20 mCi/mL. The multi-pinhole collimater we used is five pinholes, 1.0 mm aperture. After the onset of MCA occlusion and SPECT imaging, the brain was sliced coronally at 2-mm intervals, stained with TTC and the infracted area was defined. Then *ex vivo* autoradiography was performed to acquire radioactivity distribution.

Result:

Regions unstained with TTC, were observed in mice that underwent occlusion of the right MCA. Interestingly, Tc-99m –ECD SPECT imaging demonstrated that higher radioactivity was detected on the same side of ischemia compared with left hemisphere, revealed that blood flow was more active at infracted regions in our animal model. Besides, brain without ischemia had equal radioactivity distribution in right and left hemisphere. In addition, *ex vivo* autoradiography results also showed that more radioactivity on right side identically to SPECT imaging.

.

Conclusion:

Our results showed that obviously higher Tc-99m-ECD radioactivity could be detected and displayed parallel to occlusive side than non-occluded side. In conclusion, multi-pinhole SPECT imaging has excellent senstivity and high resolution to estimate infracted areas in B6 stroke animal model by Tc-99m-ECD

This study was supported by grant awarded by the department of industrial technology, Ministry of Economic Affairs, R.O.C

3D Automatic Quantitative Technique Apply to Osteoporosis Mice Study using Micro-CT Image

Yu-Ting Fang, Meei-Ling Jan *, Hung-Chin Lu, Yu-Ching Ni, Shao-Yu Peng, Teng-Kui Cheng, Lie-Hang Shen

(* Meei-Ling Jan: mljan@iner.gov.tw)

Purpose：With the development of osteoporosis diagnosis, most of the current bone mineral density (BMD) examinations adopt ordinary X-ray, ultrasound, computer tomography (CT) scan, or dual-energy X-ray absorptiometry (DEXA) inspection. A 3D automatic method to quantify the extent of bone loss using micro-CT is presented. It is expected the objective method can help the analysis of pre-clinical animal study on using xenogenic mesenchymal stem cells to strengthen osteoporotic bone.

Materials and method： The study of monitoring osteoporosis animal model is performed by using a home-made cone-beam micro-CT. 15-weeks-old, 6 normal mice and 15 mice (C57/BL6) by ovariectomy (OVX) were scanned by micro-CT at 2, 4, 6 months after surgery. X-ray source operating at 45 kV and 0.6 mA were performed for each scan. The voxel volume and image size are 100×100×100 μm^3 and 512×512×512, respectively. All the reconstructed images were processed to trace the boundary of femur head through volumetric seed growing combined with edge-following scheme. An iterative step was used to improve the accuracy of femur head segmentation. Then a special discontinuous point was chosen automatically as a threshold to distinguish the volume histogram inside the cortical bone. The volumetric ratios of threshold below to threshold above were calculated as an index for extent of osteoporosis.

Results：The results indicate that trabecular bone loss reduce average 15% to 26% for 2, 4, 6 months after OVX operation. The data was consisted with histopathology.

Conclusions: It is concluded the objective and invasive 3D imaging method for the osteoporosis evaluation of small animal is promising. The technique will apply to pre-clinical stem cell therapy studies for monitoring bone growth and repair in the future.

Keywords: Osteoporosis, Micro-CT, stem cell therapy

Study of maximum-acceptance-angle effects in positron emission mammography system

Yu-Ching Ni, Meei-Ling Jan, Hsuan-Yu Lai, Zhi-Kun Lin, Li-Ting Huang, Lie-Hang Shen
Institute of Nuclear Energy Research 325 No.1000, Wunhua Rd., Longtan Township, Taoyuan County 325, Taiwan (R.O.C.)

Dual-head positron emission mammography (PEM) system, compare to conventional PET, doesn't have data with complete angle. Therefore spatial resolution, image noise and parallax error of PEM are affected by the maximum acceptance angle. In this work, we used simulation tool to study the maximum-acceptance-angle effects on image qualities of PEM system.

The PEM system, which has two opposing detector heads with 115.2 × 192mm^2 FOV, was simulated using GATE. 3D images were implemented by the planar tomography reconstruction. Since detector-to-detector distance influence the maximum acceptance angle, to realize the effects on spatial resolution and parallax error, a 0.4mm-diameter point source was scanned with various detector-to-detector distance setups (60mm, 120mm, 200mm and 300mm). The FWHMs of PSF in 3D directions were calculated. For understanding the effect of image noise and the image blurring in practice, three 3mm-diameter lesions in digital breast phantom was scanned with previously described distance setups. One of the lesions was placed at the center of breast. The others were placed at 1.3mm left, and 4mm up from the central lesion, respectively. The activity ratio of lesion to breast tissue is all 20:1. The standard deviation of the breast tissue and the image profiles of three lesions in 3D directions will be shown.

The results show that the spatial resolutions are 1.36-1.48mm (parallel to detector plane), and 4.42-3.74mm (perpendicular to detector plane) with various detector-to-detector distance setups. Enlarge the maximum acceptance angle by closing detector heads, the blurring along direction perpendicular to detector plane is improved, however, the parallax error is increased also. The phantom results reveal the influence of acceptance angle on image quality is obvious. The scatter factor of the PEM affected by acceptance angle will be considered for further study.

Evaluation of image restoration methods for ^{188}Re quantitative micro-SPECT imaging

Shiang-Lin, Hsu, Meei-Ling, Jan, Fan-Pin, Tseng, Chung-Hsin, Yeh, Zhi-Kun, Lin, Lie-Hang, Shen

Institute of Nuclear Energy Research 325 No.1000, Wunhua Rd., Longtan Township, Taoyuan County 325, Taiwan (R.O.C.)

This study is to evaluate the effects of image restoration methods on ^{188}Re micro-SPECT images and to find the optimized parameters of these methods. Using proper restoration methods to improve the accuracy of quantitation is expected to help the analysis of pre-clinical animal experiments for ^{188}Re-(DXR)-liposome drug development.

Three restoration methods, Wiener Filter, CLS Filter and Lucy Richardson, were selected to de-blur the simulated and experimental images. The Shepp-Logan digital phantom with noise (signal-noise ratio: 2dB, 20dB, 200dB) was used to evaluate their ability of noise resistance. The images of digital phantom with noise were convoluted by degraded function of X-SPECT system to simulate the measured images. Then, restoration methods were applied on the simulated images. The results show Lucy Richardson has the best ability of noise resistance, and Wiener Filter the worst.

Various concentrations of ^{188}Re-solution (114.3, 57.2, 28.6, 14.3, 7.1 and 3.6 μCi/cc) in well plate were scanned by X-SPECT/CT (Gamma-Medica-Ideas) with high-resolution-parallel-hole collimator at time points of 0, 12, and 70 h. Reconstructed images were restored by the methods described above. The optimized parameters of Wiener Filter and CLS Filter were determined by the linearity of correlation between real activity concentration and average voxel value. Furthermore, the quantitation effect from iterative number of Lucy Richardson method was evaluated also.

It is concluded that restoration methods with proper parameters can benefit the accuracy of ^{188}Re quantitative micro-SPECT imaging.

Keywords: quantitation, image restoration, ^{188}Re-SPECT.

Quantitative 3D Micro-SPECT Imaging of ^{188}Re-BMEDA-Liposome in a C26 murine colon carcinoma solid tumor animal model

Fan-Pin, Tseng, Meei-Ling, Jan, Ya-Jane, Chang, Zhi-Kun, Lin, Shiang-Lin, Hsu, Yu-Ching Ni, Chih-Hsien Chang, Te-Wei, Lee

Institute of Nuclear Energy Research 325 No.1000, Wunhua Rd., Longtan Township, Taoyuan County 325, Taiwan (R.O.C.)

The spatial resolution of micro-SPECT with parallel-hole collimation doesn't satisfy the requirement of small animal imaging. In this study, a 3D iterative Lucy Richardson method was used to improve the accuracy of quantitative tumor-bearing mice images. The improved quantitation results were compared with biodistribution.

A Derenzo phantom (with hot regions of 0.8, 1.6, 2.4, 3.2, 4.0 and 4.8mm diameter inside) scanned by X-SPECT (Gamma Medica, USA) was used to evaluate the Lucy Richardson algorithm. The 6-section regions of interest (ROIs) and profiles were drawn on the recovered and the original images. A range of suitable iterative number was determined by comparing the full widths of half maximum and noise standard deviations.

Twenty-seven C26 mice were subcutaneously inoculated with $2x10^5$ tumor cells in the right hind flank. The animals developed tumors of about 750 mm^3 in size after tumor cell inoculation, and then the ^{188}Re-BMEDA-labelled pegylated liposomes (~0.5mCi/0.2cc) was administered to each mouse by intravenous injection. Micro-SPECT images were acquired at 1, 4, 24, 48 and 72 h after injection. Standard uptake values (SUVs) of tumor were estimated from recovered and original images. Biodistribution (5 mice for each time point) were studied for comparison.

The preliminary results reveal that the SUVs from recovered image are closer to the biodistribution studies. It is expected that image deblurring can improve the quantitation of ^{188}Re-labeled nanoliposomes images and might help to pre-clinical treatment evaluation.

Keywords: image quantitation, image recovery, micro-SPECT